CrossMark

ZNF521 Has an Inhibitory Effect on the Adipogenic Differentiation of Human Adipose-Derived Mesenchymal Stem Cells

Emanuela Chiarella[1] · Annamaria Aloisio[1] · Bruna Codispoti[2] · Giovanna Nappo[3] · Stefania Scicchitano[1] ·
Valeria Lucchino[1] · Ylenia Montalcini[1] · Augusto Camarotti[4] · Olimpio Galasso[5] · Manfredi Greco[6] ·
Giorgio Gasparini[5] · Maria Mesuraca[1] · Heather Mandy Bond[1] · Giovanni Morrone[1]

Abstract
Mesenchymal stem cells (MSCs) are multipotent progenitors present in the bone marrow stroma and in subcutaneous abdominal fat, an abundant and easily accessible source of MSCs with the ability to differentiate along multiple lineage pathways. The stem cell-associated transcription co-factor Zinc Finger Protein 521 (ZNF521/zfp521) has been implicated in the control of the homeostasis of hematopoietic, neural and osteo-adipogenic progenitors. Here we document through the analysis of a panel of human adipose-derived stem cells (hADSCs), that ZNF521 strongly inhibits the generation of mature adipocytes. Enforced overexpression of ZNF521 in these cells resulted in a significant delay and reduction in adipocyte differentiation upon exposure to inducers of adipogenesis. Of particular relevance, ZNF521 was able to inhibit the expression of ZNF423, recently identified as an essential commitment factor necessary for the generation of pre-adipocytes. Conversely, silencing of ZNF521 was found to significantly enhance the adipogenic differentiation of hADSCs. Inhibition of adipogenesis by ZNF521 was at least in part due to inhibition of EBF1. Taken together, these results confirm a role for ZNF521 as a key negative regulator of adipocyte differentiation of hADSCs.

Emanuela Chiarella, Annamaria Aloisio, Heather Mandy Bond, Giovanni Morrone contributed equally to this work.

✉ Emanuela Chiarella
emanuelachiarella@unicz.it

Annamaria Aloisio
aloisio@unicz.it

Bruna Codispoti
bruna.codispoti@tecnologicasrl.com

Giovanna Nappo
giovanna.nappo@ucsf.com

Stefania Scicchitano
scicchitano@unicz.it

Valeria Lucchino
vale.lucchino@studenti.unicz.it

Ylenia Montalcini
ylenia.montalcini@studenti.unicz.it

Augusto Camarotti
augustocamarotti@mpf.mp.br

Olimpio Galasso
galasso@unicz.it

Manfredi Greco
manfredigreco@unicz.it

Giorgio Gasparini
gasparini@unicz.it

Maria Mesuraca
mes@unicz.it

Heather Mandy Bond
bond@unicz.it

Giovanni Morrone
morrone@unicz.it

Extended author information available on the last page of the article

🖄 Springer

Background

Mesenchymal stem cells (MSCs) are multipotent precursor cells, present in bone marrow and other connective tissues, that are capable of differentiating along the chondrogenic, osteogenic and adipogenic lineages. Adipose tissue represents an accessible source of MSCs, known as adipose-derived stem cells (ADSCs). These cells have been demonstrated to have very similar phenotypic and functional characteristics to bone marrow-derived MSCs and have been proposed for several applications including bone regeneration [1, 2]. hADSCs can be isolated in large amounts from lipoaspirates or subcutaneous adipose tissue of adult subjects, propagated *in vitro* and induced to differentiate into the three mesenchymal lineages, in response to appropriate stimuli.

Adipocyte differentiation is a complex process in which preadipocytes undergo changes in cell morphology, hormone sensitivity and transcriptional events that have been studied primarily in murine preadipocyte cell lines [3]. During adipogenesis, cells convert from a fibroblastic to a more spherical shape characterized by the accumulation of cytoplasmic lipid droplets. Adipogenic commitment of early precursor cells is fine-tuned by the sequential down regulation of inhibitory and activation of a series of transcription factors that are considered key regulators of the adipocyte fate [4]. Commitment to a specific lineage appears to be mutually exclusive with alternative fates and factors that enhance adipogenesis are often inhibitory to osteoblastogenesis and *viceversa*. One critical molecule in the control of adipocyte differentiation is the master regulator Peroxisome Proliferator-activated receptor gamma (PPARγ) (reviewed in [4–7]). This nuclear receptor transcription factor is controlled positively by a variety of other transcription factors (including the CCAAT/enhancer binding proteins C/EBP, EBF1, EBF2, ZNF423, ZNF638, NF1, ADD1/SREBP1, CREB, KLF4, KLF5, KLF9, KLF15) and negatively by others (GATA2, GATA3, KLF2, PREF-1, SIRT1, TAZ). Adipocyte differentiation takes place in two waves, the first consisting of the activation of early transcription factors (C/EBP-β and C/EBPγ, KLFs, CREB, Krox20 and SREBP-1c), that in turn induce most importantly PPARγ and C/EBPα [8]. These factors act cooperatively during terminal differentiation by activating the expression of one another in a positive feedback loop, inducing growth arrest and transcriptionally regulating the expression of adipocyte-specific genes such as fatty acid binding protein 4 (FABP4), fatty acid synthase (FAS), lipoprotein lipase (LPL), stearyl-CoA-desaturase (SCD), glucose transporter type 4 (GLUT-4) and adiponectin [9, 10].

Several members of the zinc containing Krüppel-like factor (KLF) family (7 out of the 17 known KLFs [8]) have been implicated in the control of adipogenesis and are sequentially expressed during this process. In addition to this family, others

zinc finger proteins have been implicated in the control of adipocyte differentiation. In particular, ZNF423, a multifunctional Krüppel-like transcription co-factor with 30 C2H2 zinc fingers, has been identified as an essential transcriptional activator. In adipocyte precursors this factor is sequestered in the cytoplasm by WNT1-inducible-signaling pathway protein 2 (WISP2). During adipocyte commitment, BMP4 induces the dissociation of WISP2 and allows ZNF423 to enter the nucleus thereby activating the expression of PPARγ [11, 12]. ZNF423 shares high homology with another 30 ZF-containing factor, ZNF521, which was originally found as highly enriched in hematopoietic stem cells and characterized as a regulator of EBF-1 in B cell differentiation [13–16] and leukemia [17–20], and has since been found to have a central role in neurogenesis [21–23], medulloblastoma [24], osteogenesis [25–28] and chondrogenesis [29, 30].

ZNF521 and its orthologue zfp521 in mouse have recently also been implicated in the control of adipogenesis [28, 31, 32]. In *in vitro* and *in vivo* models the expression of zfp521 was correlated with the inhibition of adipogenesis of mesenchymal stem cells or pre-adipocyte cells lines via repression of Ebf-1 and of zfp423 [28, 31], as well as to increased stimulation of osteogenesis [33]. In contrast, a recent study performed on human bone marrow mesenchymal stem cells has reported that overexpression of ZNF521 enhances adipogenesis [32]. To clarify this discrepancy and better define the role of ZNF521 in the control of adipogenesis, we have undertaken an extensive study using a panel of commercially available human adipose-derived stem cells (hADSCs) and controlled differentiation conditions to determine the effect of the modulation of ZNF521 expression on hADSCs adipocytic maturation.

Results

ZNF521 Overexpression Delays Adipocyte Differentiation in hADSCs

The expression levels of ZNF521 in hADSCs were determined by Q-RT-PCR in comparison with the leukemic cell lines NB4, K562 and THP1, that express low/undetectable, intermediate and high amounts, respectively, of ZNF521 mRNA. This analysis revealed the presence in hADSCs of an intermediate level of ZNF521 mRNA, similar to that of K562 cells (Fig. 1A), that made it amenable to enforced overexpression or silencing. In addition Western Blotting analysis confirmed the same trend of ZNF521 protein expression across diverse cell lines (Fig. 1B).

To enhance ZNF521 expression we infected hADSCs with a lentivirus termed FUIGW-ZNF521, containing an expression cassette comprising the strong promoter of the
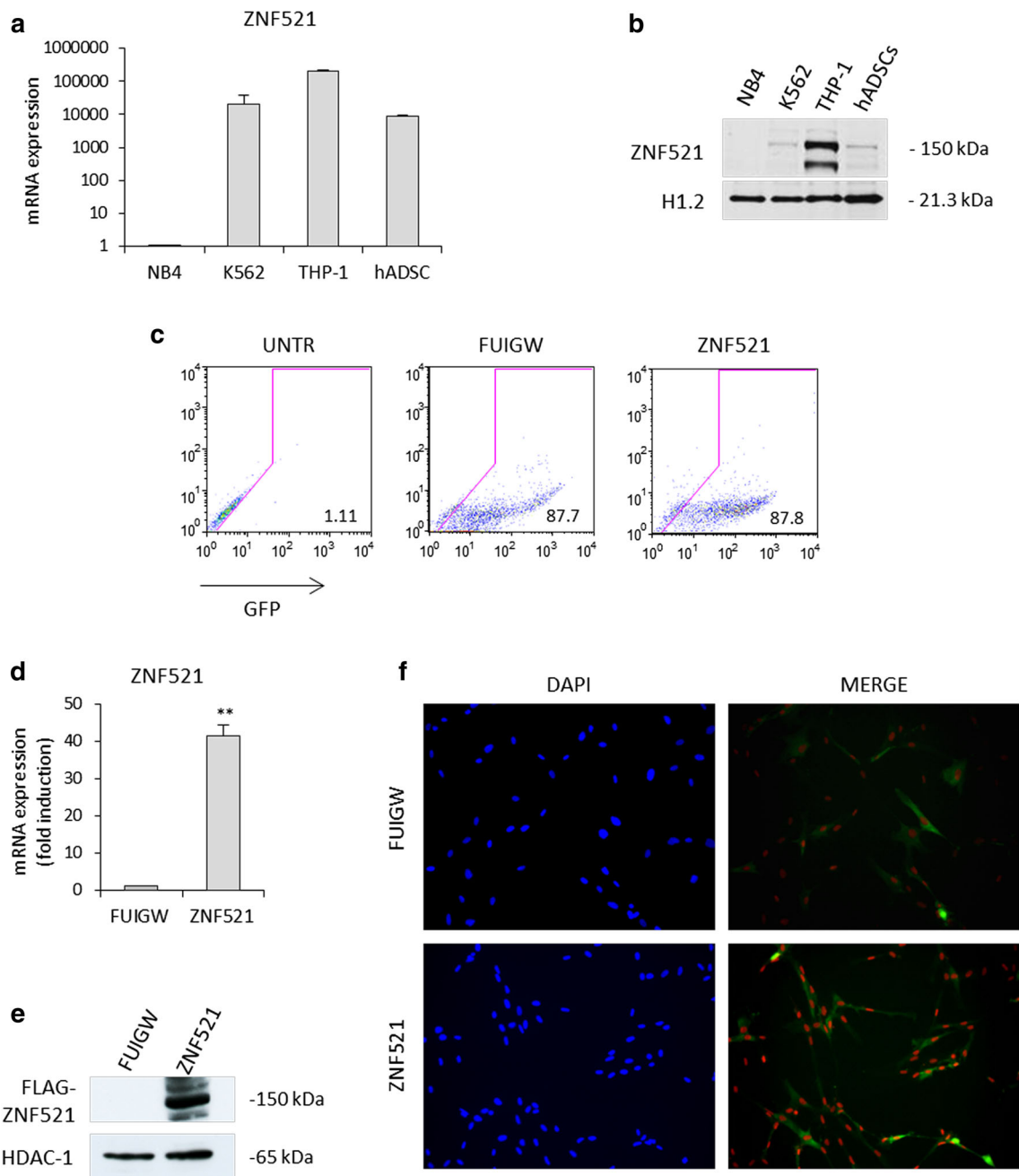
Fig. 1 Analysis of ZNF521 overexpression in hADSCs. (**A**) Q-RT-PCR was used to quantify the mRNA levels of endogenous ZNF521 in cultured hADSCs and in the low, intermediate and highly expressing hematopoietic cell lines: NB4, K562 and THP1 (**B**). Western Blotting analysis with nuclear extracts showed endogenous ZNF521 protein expression in the four different cell types. (**C**). Lentiviral mediated transduction was used to introduce ZNF521 with the eGFP reporter gene. Flow cytometry was performed on day 3 for eGFP and for ZNF521 and control (FUIGW) transduced cells. (**D**) Q-RT-PCR of cells transduced with the FUIGW-ZNF521 vector showed up to a 40-fold increase of mRNA. (**E**) Western Blot analyses with nuclear extracts shows introduction of Flag-ZNF521 detected with anti-Flag antibody, normalized for the HDAC-1 nuclear protein. (**F**) Immunofluorescence with rabbit anti-ZNF521 antibody detected with Alexa fluor 594, showed an increased signal in the ZNF521 transduced cells compared to low levels of endogenous nuclear ZNF521. Nuclei were stained with DAPI and counter stained with mouse anti-actin detected with Alexa fluor 488.

Ubiquitin C gene (UBC) [34], the ZNF521 coding sequence, an intra-ribosomal entry site (IRES) sequence, and the cDNA for the reporter fluorescent protein eGFP. This vector allows the simultaneous expression of transgene and reporter protein, encoded by a single bi-cistronic mRNA [35].

FACS analysis, performed to assess the transduction efficiency on hADSCs exposed to FUIGW-ZNF521 or to the control void virus FUIGW, confirmed a high transduction rate and high expression of eGFP (> 85%) (Fig. 1C). The levels of ZNF521 transcript, as measured by Q-RT-PCR, were

increased by approximately 40-fold in the transduced cells (Fig. 1D). The expression of Flag-ZNF521 protein was confirmed by Western Blotting in nuclear extracts using an antibody to the Flag-tag fused to its coding sequence (Fig. 1E). Immunofluorescence analysis using an antibody against the endogenous protein showed that ZNF521 displayed a strongly enforced expression compared to the control cells and accumulated in the nuclei of the cells transduced with FUIGW-ZNF521 (Fig. 1F).

To investigate the effects of ZNF521 overexpression in hADSCs, cells were stimulated to differentiate along the adipogenic lineage with defined commercial medium for adipocyte differentiation (Life Technologies). hADSCs induced towards adipocytes were characterized by the appearance of intracellular lipid droplets (LDs) visible by phase contrast microscopy. To monitor the adipogenic stages of differentiation, Oil red O staining was performed on day 7 and 14 after induction. Seven days after adipogenic induction, we observed that the size and amount of stained LDs, mainly visible in the perinuclear region, were considerably smaller in ZNF521-transduced cells, compared to the cells transduced with control FUIGW vector which had accumulated visibly more LDs. By day 14, the LDs had increased in staining intensity and filled most of the cytoplasm surrounding the nuclei. Untreated cells instead displayed little or no lipid accumulation (Fig. 2A).

To monitor the influence of ZNF521 on components of the molecular mechanisms underlying adipogenesis, the expression of a set of adipogenic markers was measured by Q-RT-PCR on day 3, 7, and 14. While the expression of endogenous mRNA was found to decrease moderately during the later stages of adipocyte differentiation (Fig. 2B), ZNF521 overexpression was associated to a significantly lower induction of the major adipocyte transcription factors PPARγ and C/EBPα, evident already after 3 days of differentiation and this inhibitory effect was maintained during the differentiation (Fig. 2B and Additional files 1A-1B). The cognate transcription co-factor ZNF423 was moderately induced following the exposure to adipogenic stimuli by 7–14 days and this induction was completely suppressed by enforced overexpresssion of ZNF521. Additionally the adipocyte transcription factor C/EBPβ was monitored by immunofluorescence staining after 10 days of adipocyte differentiation. The typical sub-nuclear distribution of C/EBPβ was evident and this too was markedly reduced in ZNF521-transduced cells (Fig. 2C) compared to control cells. The expression of PPARγ and C/EBPα and target genes such as FABP4 and LPL, were also found to be dramatically up-regulated in stimulated hADSCs and strongly delayed and reduced in their counterpart over expressing ZNF521 (Fig. 2B and Additional files 1A-1B).

In a parallel approach hADSCs were transiently transfected by nucleofection with ZNF521 and the expression analyses were performed prior to the stimulation and after 5 days of adipogenic stimulation. At latter time points the ZNF521 over

Fig. 2 Inhibitory effect of ZNF521 ectopic expression on adipocyte ▶ differentiation in hADSCs. (**A**) hADSCs were cultivated in complete proliferation medium 14 days (Non Induced, NI) or induced to differentiate and stained with Oil Red O on day 7 and 14 and visualized by phase contrast microscopy. The amount of lipid droplet formation was markedly less in ZNF521 transduced cells compared to control FUIGW cells. Intracellular lipid droplets were not detectable in control cells cultured in complete proliferation medium for 14 days (experimental replicate $n = 3$). Representative images are shown magnification 20×. (**B**) Q-RT-PCR analysis of gene expression normalized for the housekeeping genes GAPDH or UBC. ZNF521 mRNA was modestly down regulated during differentiation by 7 and 14 days. ZNF521 over expression results in the reduced and delayed expression of adipocyte specific transcription factors ZNF423, PPARγ, C/EBPα and markers FABP4 and LPL. Data are represented as means ± SD from a representative experiment performed in duplicate (* $p < 0.05$). (**C**) Representative brightfield and immunofluorescence images showing adipocyte differentiation at day 10 where cells were stained with C/EBPβ antibody (red) and nuclei blue DAPI, magnification 20× (experimental replicate $n = 2$).

expression, although reduced, was still evident, and resulted in a significant repression of the expression of PPARγ, C/EBPα and ZNF423 as well as FABP4 and LPL (Fig. 3A). Oil Red O staining was performed on transfected cells after 7 days of induction. The results showed that ZNF521 is able to prevent adipocyte differentiation/maturation: cytoplasmic lipid droplets accumulation was almost completely blocked in hADSCs overexpressing ZNF521 compared to control cells (Fig. 3B).

Thus, as shown in Figs. 2 and 3, both transient or stable enforced expression of ZNF521 resulted in a considerable attenuation of hADSCs differentiation toward adipocytes both at the morphological and at the molecular level. This is confirmed by the results shown in Additional files 1A and 1B, that summarize a complete set of 6 experiments with distinct individual lots of hADSCs. In all these experiments, despite the expectable individual variability in the kinetics and rate of differentiation, ZNF521 overexpression was invariably associated to a significant inhibition of hADSC adipogenesis.

ZNF521 Silencing Facilitates Differentiation in hADSCs

In a complementary approach, we sought to establish whether the knock-down of ZNF521 in hADSCs would induce an opposite effect from its overexpression. To this end, ZNF521 silencing was performed using lentiviral vectors carrying two distinct ZNF521-specific shRNAs, previously shown to effectively reduce the protein expression [15, 16, 24, 35]. The high efficiency of the lentiviral transduction in hADSCs was evident by FACS analyses of eGFP (Fig. 4A) and then the silencing was verified by Western Blotting, using an antibody against endogenous ZNF521. As shown in Fig. 4B, transduction with lentiviruses carrying both ZNF521 shRNAs (shRNA-1 and
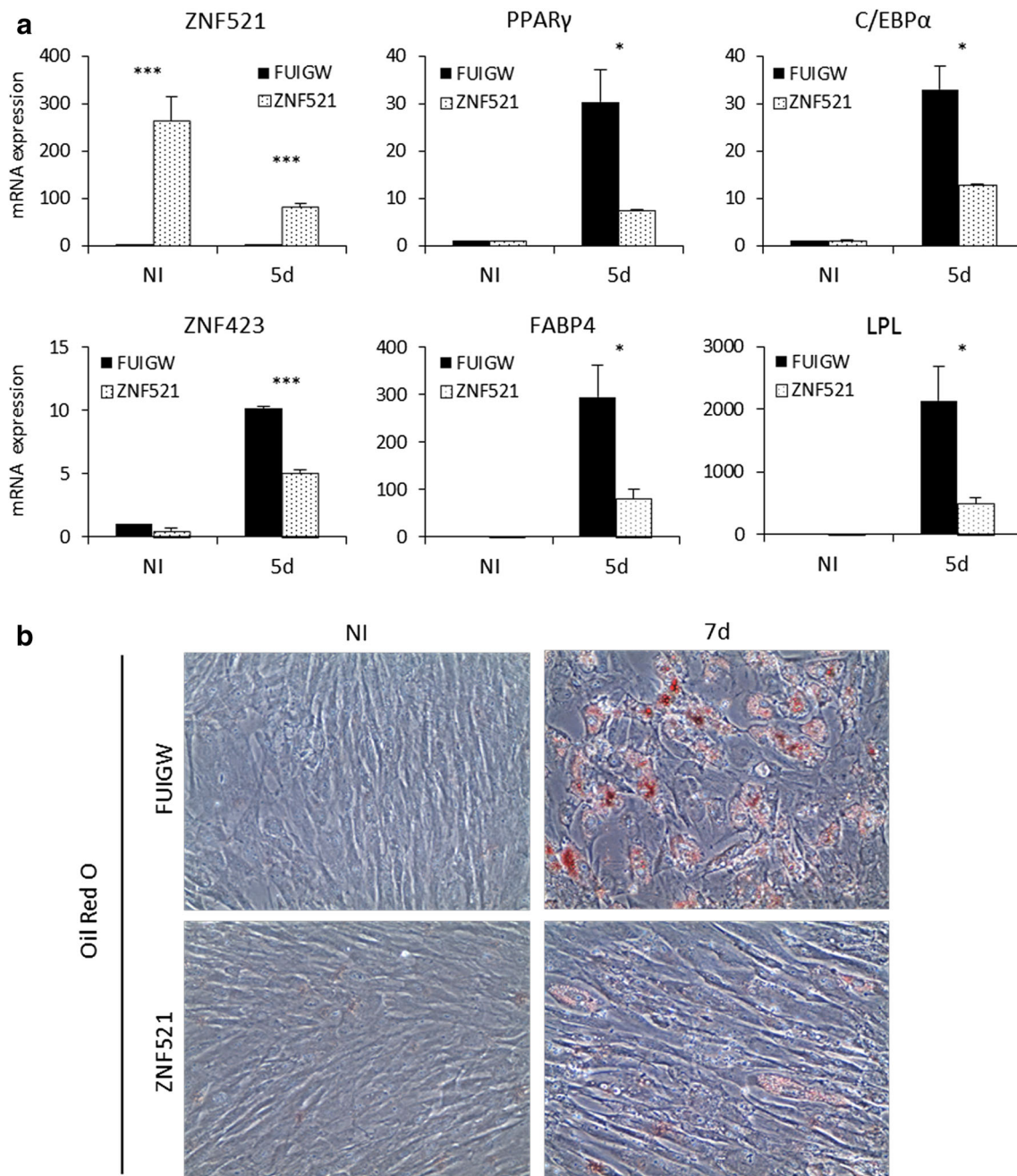
a

b
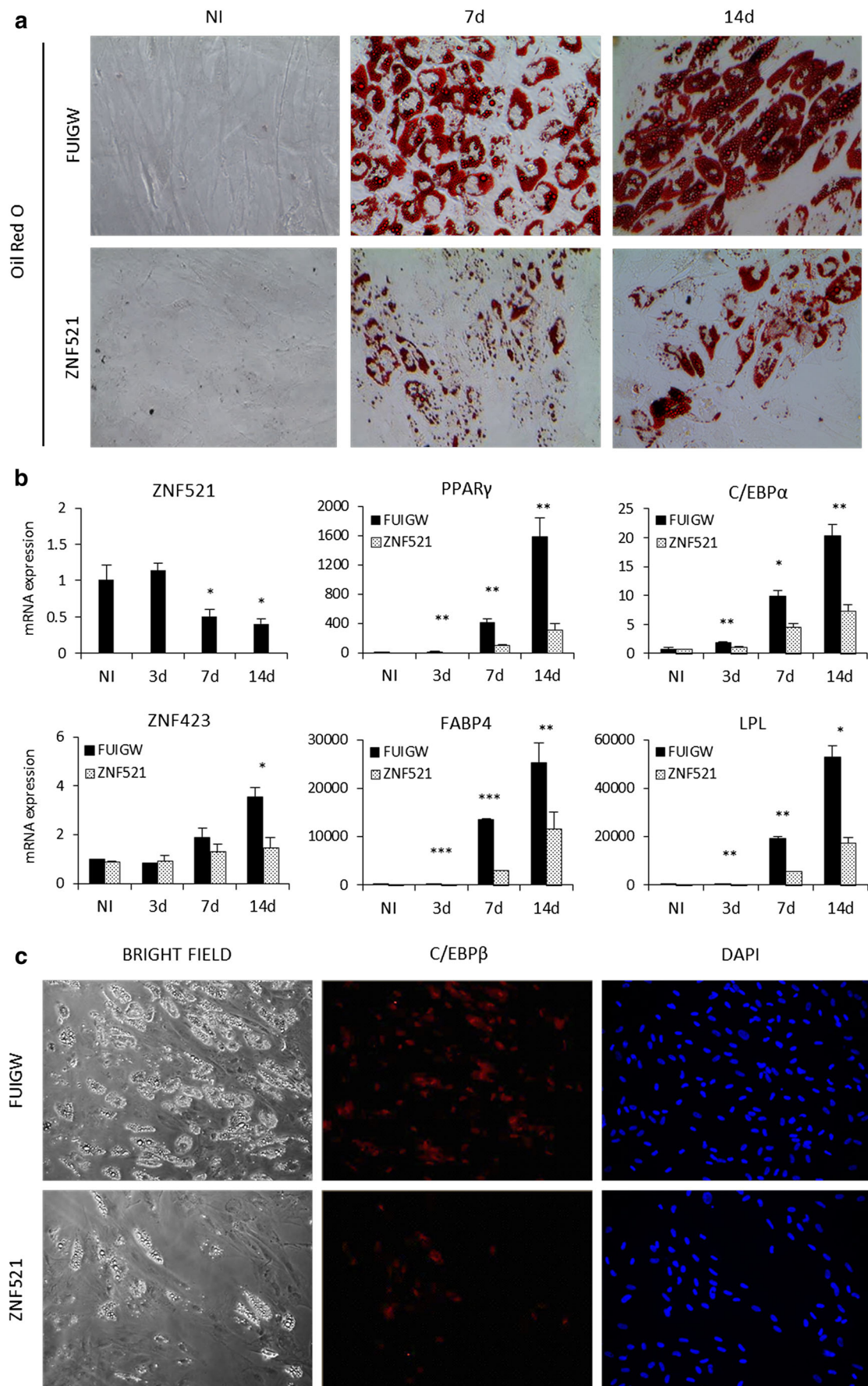
Fig. 3 Effects of transient ZNF521 overexpression. (**A**) hADSCs were transfected by nucleofection and cultured in the adipogenic medium for 5 days. mRNA transcript levels of specific adipocyte-related genes were analysed by Q-RT-PCR and their expression levels are reduced compared to control cells (replicate $n = 3$). Student's t-test was used for statistical analysis (* $p < 0.05$). (**B**) hADSCs transfected with ZNF521 were analysed by Oil Red O staining to evaluate cellular morphological modifications and intracellular lipid accumulation by 7 days after the induction of adipocyte differentiation. This experiment was performed twice.

shRNA-2) abrogated almost completely endogenous ZNF521 protein expression compared to the shRNA control vector. In addition, Q-RT-PCR showed that the level of ZNF521 mRNA was significantly reduced in shZNF521-transduced cells compared to the negative control (Fig. 4C).

ZNF521-silenced hADSCs were treated with adipocyte inducers for 14 days and stained with Oil Red O, at 7 and

14 days. Morphological examination showed that the number of LDs and their intensity of staining was enhanced in ZNF521-silenced cells compared to shRNA no-target control (Fig. 5A). Concomitantly the expression of the transcription factors PPARγ, C/EBPα and ZNF423 as well as the adipocyte specific FABP4 and LPL genes during differentiation was markedly enhanced in the ZNF521-silenced hADSC cells compared to control cells at all stages of analysis (Fig. 5B
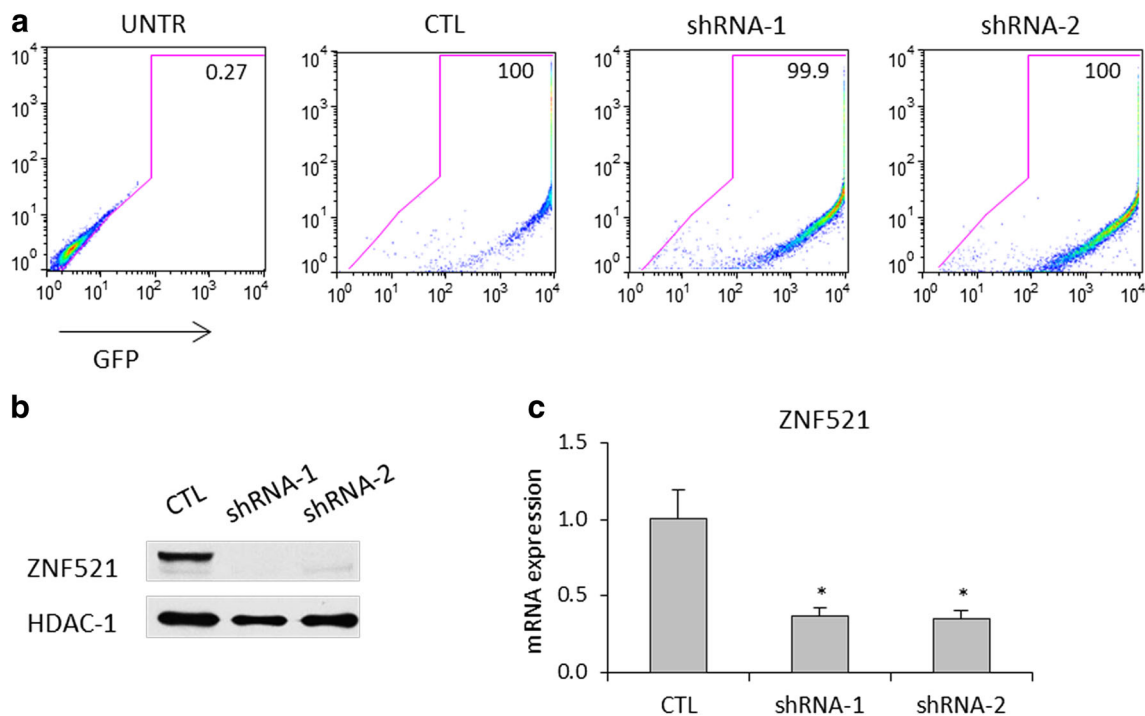
Fig. 4 Analysis of ZNF521 silencing. (**A**) ZNF521 was silenced using a lentiviral shRNA strategy and the efficiency of eGPF trans gene transduction was evaluated by flow cytometry. (**B**) Silencing was confirmed by western blot analysis of ZNF521 protein. (**C**) Q-RT-PCR analyses shown that mRNA levels of ZNF521 were reduced by at least >50%.

and Additional files 2A-2B). Immunofluorescence staining for C/EBPβ protein in hADSCs differentiated cells showed greater positivity in the sub-nuclear region of ZNF521-silenced cells (Fig. 5C). This was the case for all the six hADSC samples studied (Additional files 2A-2B) where a highly efficient adipocyte differentiation accompanied by an increased expression of adipocyte marker genes being consistently associated with ZNF521 silencing. Thus, silencing of ZNF521 results in an opposite effect on adipocytic differentiation of hADSCs compared to ZNF521 overexpression, and consistently accelerates this process in response to appropriate stimuli.

## Quantification of Oil Red O Staining Using an ImageJ Based Method

In order to gain additional quantitative information on the effect of ZNF521 on adipogenic differentiation an ImageJ based method was applied. The results were summarized in the additional file 3. The data presented on the bar graphs confirmed that ZNF521 was able to modulate adipocyte differentiation; in the cells overexpressing ZNF521 the mean of the Oil red O stained area, calculated as a percentage of each field and the mean of the red intensity (pixels), after 7 and 14 days, was significantly decreased compared to control cells. It could be calculated that in the final phase of differentiation, ZNF521 overexpression reduced the area covered by

the stain and the red intensity by approximately five times (Additional file 3A).

Consistently, in cultures of ZNF521 silenced cells the difference in stained covered area and red intensity was increased in a progressive manner in both ZNF521 shRNA transduced cells compared to controls. On the 14th day, it was observed that the area covered by the stain and the red intensity of the staining was approximately 6.5 times higher compared to those of control cells (Additional file 3B).

ZNF521 Acts by Inhibiting EBF-1

ZNF521 is known to act as a potent inhibitor of early B cell factor 1 (EBF-1), considered a master factor of B cell differentiation [15] and a prominant inducer of adipocyte differentiation [31, 36, 37]. ZNF521 binds to EBF-1 through its C-terminal domain and counteracts the transactivation of several EBF-1 target genes involved in B-lymphopoiesis and as well as in adipogenesis. EBF-1 is known to be a potent activator of PPARγ [38]. The activity of PPARγ can be assayed by measuring the transcriptional activation of a reporter plasmid in which the expression of the luciferase gene is under the transcriptional control of PPARγ (PPRE-luciferase reporter, Cignal Qiagen reporter, which contains repeated elements of the PPARγ binding consensus from the ACOX1 gene) [39]. We tested if overexpression of EBF-1, zfp521 or both in the

a

b

c
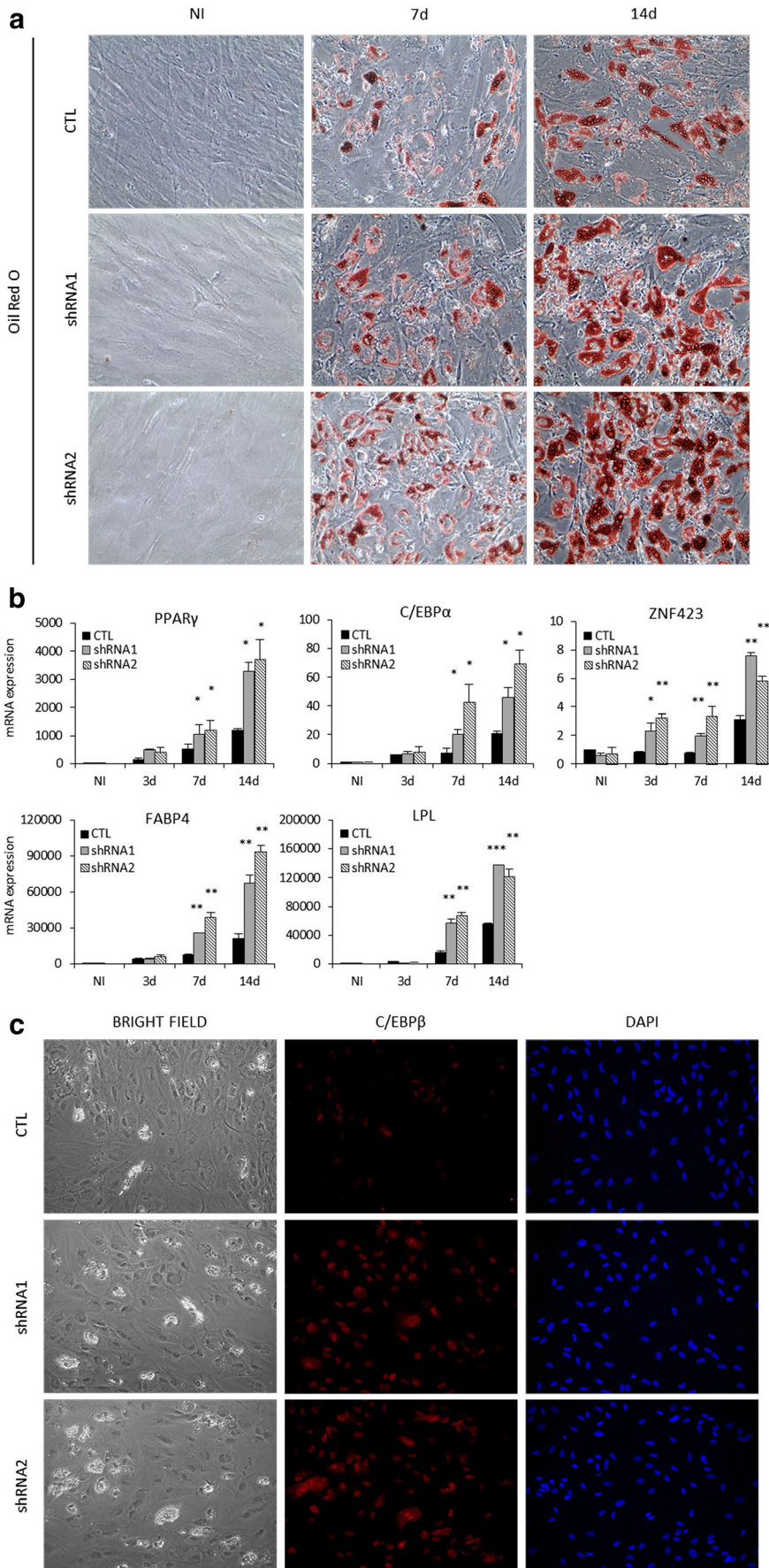
◀ **Fig. 5** Silencing of ZNF521 promotes human adipocyte differentiation. (**A**) ZNF521 silencing significantly enhanced the number of lipid accumulation in hADSCs which were stained with Oil Red O on 7d and 14d. All assays were performed at least in duplicate. (**B**) Q-RT-PCR analyses shows that ZNF521 silencing enhances the induction of the expression of the main characteristic adipogenic transcription factors and marker genes. Values are from duplicate. (**C**) Immunofluorescence staining shows differentiated hADSCs on day 10. The appearance on differentiation of C/EBPβ protein was more evident in the cells transduced with shRNAs compared to shRNA control vector (CTL). Each staining was made in duplicate. Representative images are shown with subnuclear localization of C/EBPβ (red) and DAPI (blue), (magnification 20×).

preadipocyte mouse cell line, NIH3T3-L1, would affect the expression of this PPARγ reporter construct. To this end, NIH3T3-L1 cells were transfected with the PPRE-luciferase reporter together with control vector, zfp521, EBF-1 or both. As shown in Fig. 6 overexpression of zfp521 significantly decreased the luciferase expression driven by the PPRE element both in basal conditions and in the presence of EBF-1 suggesting that its inhibitory effect on hADSCs is, at least in part, due to interference with the EBF-1 induced activation of PPARγ driven transcription [38].

Discussion

Human adipose-derived stem cells represent a readily available supply of mesenchymal stem cells with the ability to undergo osteogenesis or chondrogenesis and are susceptible to generate lipid laden adipocytes. Adipocyte differentiation can be achieved with dexamethasone (DEX), insulin, isobutyl-methylxanthine (IBMX) and indomethacin with in some protocols the addition of PPARγ agonists (such as rosiglitazone) [1]. In the present paper a commercial
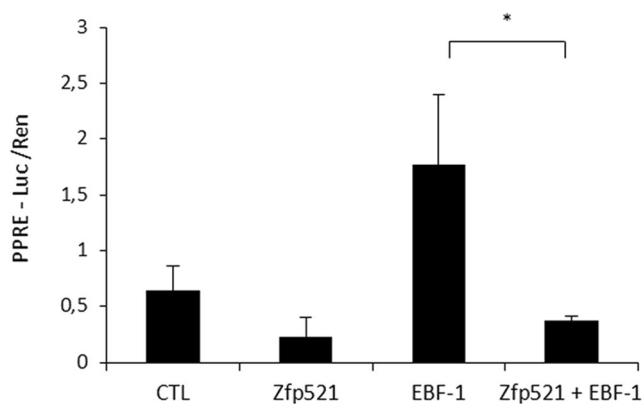

Fig. 6 Differential activation of PPRE responsive element by zfp521, EBF-1 or by both together. NIH3T3-L1 cells were transiently transfected with the PPRE responsive element construct, in presence of plasmids for zfp521 or EBF-1 or with both; as a control the void vector FUIGW was also transfected. After 48 h the luciferase activities were measured by using the Dual-Glo Luciferase Reporter Assay Kit (Promega). This experiment was repeated three times with similar results.

standardized adipocyte medium (STEM PRO® adipogenesis differentiation medium from Life Technologies) proved to result in efficient adipogenic differentiation in 7 days approssimately.

The transition from a fibroblast-like phenotype to pre-adipocytes and eventually to mature adipocytes is controlled by a series of epigenetic events and key transcription factors, in turn regulated positively or negatively by a series of additional "molecular rheostats" [1] that composing a fine-tuned molecular network, to achieve the appropriate molecular events required to attain the final differentiation. This has implication both in development and also in the homeostasis of adipose tissue in normal conditions or diseases, for example obesity. Therefore a better understanding the mechanisms that control adipogenesis may shed relevant insight for this process and also help identify potentially useful therapeutic targets for metabolic disorders. Several lines of evidence suggest that Zfp521 acts as a repressor of adipogenesis *in vitro* and *in vivo* [31]. Overexpression of Zfp521 in mouse pre-adipocytes has been postulated to inhibit their adipogenic potential, whereas its knock-down enhances differentiation. Zfp521 has been reported to exert this role by interacting with Ebf1 and inhibiting its transcriptional activity of the pre-adipogenic transcription co-factor Zfp423, while directly repressing the promoter of this gene [28].

A significant variance with these reports, Tseng et al. [32] using human bone marrow derived mesenchymal stem cells (bmMSCs) and C3H10T1/2 cells, reported that ZNF521 expression enhances adipocyte and represses osteoblastic differentiation. The expression of mRNA for ZNF521/zfp521 was found in hADSCs to be moderately down regulated during differentiation, this trend is fully consistent with that observed in C3H10T1/2 cells [31] whereas a more definite down-regulation was seen in W20–17 murine bone marrow stromal cells [28] and by Western blotting in NIH3T3-L1 cells. The rate of decline of ZNF521 in adipocytes will depend largely on the induction of Zfp423 will then act to repress the zfp521 promoter [28] and also on post-transcriptional regulation on the zfp521 protein itself. In contrast Tseng et al. [32] observed a reduction in osteoblastic differentiation and an increase during adipogenic differentiation in C3H10T1/2 cells with Zfp521 overexpression. Whether this apparent discrepancy is due to a different cellular and molecular context in which the studies have been performed is not completely clear. To determine the effect of ZNF521 in the early differentiation we used hADSCs as the most physiologically relevant model to study human adipogenesis. The experiments were performed using a panel of distinct populations of hADSCs in which the effects of up- or down-regulation of ZNF521 were analyzed using morphological and molecular parameters. The results of this study, illustrated in Figs. 1, 2, 3, 4 and 5 and in additional file 1A, clearly confirm that

overexpression of ZNF521 consistently and significantly reduced and delayed the differentiation of hADSCs to adipocytes. Conversely, its silencing resulted in enhanced and accelerated differentiation.

Interestingly, there is a recent report using the rat model of maternal food restriction (MFR) and analysis of bone marrow mesenchymal cells from the offspring, where there was a marked increase in obesity and an altered metabolic phenotype compared to normally fed animals [40], indeed these MFR bmMSCs coherently expressed reduced levels of the runx2 and zfp521 inhibitory transcription factors. This would be consistent with the idea that these transcription factors are controlling early events in adipocyte progenitor pre-programming and only once their expression decline the differentiation program can proceed. These results also predict that there may be considerable differences in the adipogenic ability of ADSCs from different tissue sources and derived from varying previous or actual metabolic regimes. Indeed we observe a considerable variation in the rate of adipocyte generation with the different ADSC donors; even so however, the influence of ZNF521 overexpression or silencing was always consistent with an inhibitory adipocyte transcriptional role.

It will be interesting in future studies to test whether the biological effects of ZNF521 may differ in MSCs from other origins. Given the complexity of the transcription networks that have been proposed [5–9] to promote and regulate differentiation, qualitative and/or quantitative variations in the composition of these networks in cells of diverse origin may significantly alter their biological activities.

Indeed, ZNF521 has been shown to interact with several other transcription factors and epigenetic modifiers in different cellular contexts including EBF-1 in B cells [16] GATA1 in erythroid progenitors cells [41], Runx2 in osteoblasts [27], p300 during neural differentiation of embryonic stem cells [21] as well as Smad proteins in response to BMP4 signaling [13]. In addition, a strong interaction of ZNF521 has been observed with the NuRD complex [14, 41] as well as with itself and Zfp423 [42, 43].

An additional wealth of information confirms the involvement of ZNF521 in MSC maturation and experiments where the constitutive activation of PDGFRα V561D resulted in the inhibition of embryonic white adipose tissue organogenesis and was accompanied by a specific upregulation in zfp521 expression (not that of zfp423 or ebf1) which in turn transcriptionally blocks adipogenesis [44]. In addition the translation control of Zfp521 may also play an important role as shown by the proteasomal degradation of zfp521 mediated by the Siah2-ubiquitin ligase in response to BMP4 during adipogenesis [45]. The functional significance of these molecular interactions and signaling processes operating to control the cell fate decisions in MSCs point to a role for ZNF521/zfp521 as an essential key upstream transcription factor for adipogenesis, whose regulation is under fine control.

Methods

Cell Culture

STEM PRO® Human Adipose-Derived Stem Cells (hADSCs) were purchased from Life Technologies (cat. no. R7788–115). Each vial (1×10^6 cells) originated from a single donor of human lipo-aspirate tissue. hADSCs ($n = 4$) were cultured in MesenPRO RS™ medium (cat. no. 12746–012 Life Technologies), containing 1X Glutamax (Life Technologies). Human hematopoietic cell lines NB4, K562, THP-1 were cultured in RPMI 1640 medium, and HEK 293 T and NIH3T3-L1 cells were cultured in DMEM. Media were supplemented with 10% fetal bovine serum. All cells were cultivated in 50 U of penicillin and 50 μg of streptomycin/ml at 37 °C in 5% CO_2.

Expression Vectors

The lentiviral vectors FUIGW-ZNF521, FG12-H11 (shRNA-1) (GCUAAAGAUAGUAAUGCATT) and FG12-H12 (shRNA-2) (UGUGGAACAAAUGGAGCUUTT) have been previously described [24, 46]. For silencing experiments, the non-target Mission lentiviral vector (Sigma) was used as control vector.

Lentiviral Particles Production and Transduction

Lentiviral particles were obtained by transient transfection of HEK293T cell line, used as a virus producing cell line. 10 μg of transfer vector were co-transfected with 10 μg of pCMV vector Δ8.9 and 2 μg of VSVG vector (Vesicular Stomatitis Virus Glycoprotein), encoding for the envelope and the packaging genes respectively, in 2×10^7 HEK293T cells using calcium phosphate precipitation [47]. After 6 h incubation at 37 °C the medium was changed and DMEM 3% FBS was added. Supernatant containing the viral particles was collected 24 and 48 h after transfection, filtered (0.45 μm cellulose acetate) and added to $2,5 \times 10^5$ hADSCs. The repetition of 2 consecutive cycles of spin inoculation (700 g at 32 °C for 40 mins), in the presence of 8 μg/ml of polybrene (Sigma), gave a high efficiency of transduction.

Flow Cytometry

Transduction efficiency was assessed using flow cytometry. Enhanced green fluorescent protein (eGFP) expression was measured using BD FACScan™ System (Becton Dickinson) and analyzed by FlowJo software. Untransduced hADSCs were used as a negative control sample.

Protein Extracts

Cytosolic and nuclear extracts were prepared essentially as described by [48], from 3×10^6 cells after washing twice with PBS. The cell pellets were resuspended in a hypotonic lysis buffer containing 10 mM Hepes pH 7.9, 10 mM KCl, 0.1 mM EDTA pH 8.0, protease inhibitors (P8849, Sigma) and phosphatase inhibitor cocktails 2 and 3 (P0044, P5726 Sigma) and incubated on ice for 20 min. Igepal-630 (NP40) 0.25% was added to cell lysates and samples were then centrifuged for 15 min at 14,000 g to clear lysate cytosolic extract. The pelleted nuclei were extracted in a hypertonic buffer containing 20 mM Hepes pH 7.9, 0.4 M NaCl, 1 mM EDTA pH 8.0, protease and phosphatase inhibitors. The lysates were subjected to three rounds of alternating vortex mixing and ice-cooling, and then were centrifuged at 15,000 g for 20 min and the supernatants (nuclear extracts) were collected.

To obtain the total protein extracts, cells were resuspended in lysis buffer (250 mM Tris-HCl pH 7.5), and then subjected to three cycles of freezing and thawing (−70/+37 °C). The lysate was centrifuged at 15,000 g for 20 min and the supernatants containing the whole-cell extracts was recovered [35].

Protein concentrations were measured from the cell lysates using the Bradford assay at 595 nm, with bovine serum albumin (BSA, Sigma) as a standard.

Western Blotting Analysis

Protein extracts (30 μg) were re suspended in 1× NuPAGE sample buffer, denatured at 95 °C for five minutes and separated by electrophoresis on 4–12% NuPAGE Novex bis-Tris gradient polyacrylamide gels (Life Technologies). Proteins were transferred to nitrocellulose membranes (0.45 μm) for 2 h at 50 V in 25 mM Tris, 192 mM glycine. Electrophoresis and blotting quality were checked by staining the membrane with 0,1% Ponceau S in 5% acetic acid and were blocked using 5% milk powder in PBS-0.05% Tween20 before incubating with antibodies. The HRP-conjugated anti-FLAG monoclonal antibody (M2 A8592, Sigma-Aldrich) was used at a 1 : 10,000 dilution for the detection of FLAG epitope-tagged proteins. Anti-HDAC-1 (H3284 - Sigma) and Anti-H1.2 (ab4086 - Abcam) were used at 1 : 12,000 and 1:10,000 respectively and were detected with anti-rabbit secondary HRP-conjugated antibody (Santa Cruz, Biotechnology). A rabbit antibody against ZNF521 (S-15 EHZF antibody - Santa Cruz Biotechnology) was used 1:1000 dilution, in non-reducing conditions, to detect the endogenous expression of ZNF521. HRP was revealed using the ImmunoCruz Western blotting luminal reagent (Santa Cruz, Biotechnology) by autoradiography.

Adipocyte Differentiation

hADSCs were confirmed positive for CD73, CD90, CD105 and negative for CD14 and CD45 by FACS and at the third passage were seeded in 12 well plates at the density of 1×10^4 cells/cm^2. To induce differentiation, confluent cells were incubated for 14 days with STEM PRO® adipogenesis differentiation medium (cat. no. A1007001 Life Technologies). Control cells were cultured in MesenPro RS™ medium (Life Technologies). The protocol was applied to hADSCs from 4 different lots. Cells were maintained at 37 °C in a 5% CO$_2$ incubator and the medium was changed every 3 days. Following a 2 week period of stimulation, the cells were stained with Oil Red O.

Oil Red O Staining

Cells were washed twice with PBS, fixed with 10% formaldehyde for 15 min at −20° C and washed twice with PBS and then stained for 30 min at room temperature in freshly diluted Oil Red O Solution (O1391- Sigma; 0.5% in isopropanol diluted with double distilled water and filtered using 3 mm Whatman paper) and then washed twice with distilled water. Images were acquired using an inverted microscope Evos (Life Technologies).

For quantification the images were processed using the software ImageJ (NIH Image Bethesda, MD). The calculation of the area was accomplished by selecting the pixels which the red component on a 24-bit RGB representation is higher than the other color components (blue and green). In this way, the percentage of the area covered by the Oil Red O stain is the number of pixels selected divided by the total pixels of the entire image (experimental replicate $n = 3$).

RNA Isolation

RNA extraction from hADSCs was performed according to the instructions of the TRIzol reagent (Life Technologies). RNA was resuspended in 20 μl nuclease-free water. The concentration and purity of the RNA was determined using the NanoDrop 2000/2000c Spectrophotometer (Thermo Fisher Scientific). The RNA quality was monitored using 1.5% agarose gel run in 0.4 M MOPS pH 7.1 (MOPS: 3-(N morpholino)propanesulfonic acid), 0.1 M NaAc, 20 mM EDTA).

Q-RT-PCR Analysis

cDNA was synthesized from 1 μg RNA using SuperScript III reverse transcriptase at 42 °C and 2.5 μM random hexamers (Life Technologies). Q-RT-PCR reactions were carried out with the iQ™ SYBR® green super mix (Bio-Rad) in duplicate according to the manufacturer's instructions and analyzed using

iQ5 multicolor detection system (Bio-Rad). One cycle of 3 min at 95 °C was followed by 45 cycles of 10 s at 95 °C, 10 s at 60 °C and 20 s at 72 °C and then a melting curve. Relative gene expression was determined using the comparative threshold cycles Ct method, normalizing for endogenous GAPDH or ubiquitin C (UBC) and expression ratio was calculated as 2^{-ddCt}, essentially as described in [16] (experimental replicate $n = 2$). Primers used for Q-RT-PCR are listed in Table 1, oligonucleotide primers were designed to detect the adipocyte-specific marker PPARγ2.

Immunofluorescence

Immunofluorescence was performed essentially as described in [24]. hADSCs were washed three times with PBS and fixed with 4% paraformaldehyde for 20 min at 4 °C. The cells were permeabilized with 0.3% Triton X-100 for 5 min and then were rinsed 3 times with cold PBS before incubating with blocking buffer (PBS, 10% BSA (Albumin Fraction V A1391 – Applichem), 0,2% Tween-20) for 40 min at room temperature. Rabbit anti-ZNF521 (HPA023056 - Sigma), mouse anti-actin (A4700 Sigma) and rabbit anti-CEBP β (C-19: sc-150 Santa Cruz Biotechnology) primary antibodies were diluted 1:500 in blocking buffer and cells were incubated with the antibody overnight at 4 °C. The cells were then washed with cold PBS three times, and incubated with Alexa fluor 488-labeled anti-mouse or Alexa fluor 594-labeled anti-rabbit secondary antibodies (Life Technologies) diluted 1:800 in blocking buffer (PBS, 2% BSA, 0,2% Tween-20) at room temperature for 1 h. Nuclei were stained with 10 ng/ml DAPI in PBS for 5 min. Cells were visualized and images were captured with

a DFC 3000 G camera mounted on a Leica Microscope (DM IL LED) at a 20× magnification.

Transfection

Cells (8×10^5) were transfected by Amaxa Nucleofector (Lonza) according to the instructions of the provider. Cells were nucleofected using the appropriate solution/program: NIH3T3-L1, V/C-023; hADSC, Human MSC Nucleofector Solution/U-23. Adherent cells were seeded for 24–48 h prior to induction of adipocyte differentiation or transactivation luciferase assays.

Luciferase Reporter Assay

NIH3T3-L1 cells were transiently co-transfected using Nucleofector technology with the PPRE-responsive luciferase construct (Qiagen CCS-3026 L) and the empty FUIGW plasmid or the plasmids FUIGW-Zfp521 and EBF-1 alone or in combination. After 48 h, luciferase activity in total cell lysates was measured using the Dual-Glo luciferase assay system (E2920 Promega) according to manufacturer instructions. Luminescence was measured using GloMax-96 Microplate Luminometer (Promega).

Statistical Analysis

The experimental data are reported as means ± standard deviation (SD). In all Q-RT-PCR figures, bar graphs represent means and error bars represent SD. Student's t-test was used for statistical analyses (* $p < 0.05$ were considered statistically significant).

Compliance with Ethical Standards

Conflict of Interest The authors declare that they have no competing interests.

Abbreviations ZNF521, Zinc finger protein 521; MSCs, Mesenchymal Stem Cells; hADSCs, human Adipose-Derived Stem Cells; ZNF423, Zinc finger protein 423; EBF-1, Early B Cell Factor-1; PPARγ , Peroxisome Proliferator-Activated Receptor gamma; C/EBPs , CAATT/ enhancer binding proteins; EBF-2, Early B Cell Factor-2; ZNF638, Zinc

Table 1 Oligonucleotide primers used in this study

Human genes	
ZNF521	FWD TGGGATATTCAGGTTCATGTTG
	REV ACTGGAGTTTGGCAGGAGAG
ZNF423	FWD GGAAAGGCACCCAGACATCG
	REV CGGGGAGTCGAACATCTGGT
FABP4	FWD TGGGCCAGGAATTTGACGAA
	REV GACGCATTCCACCACCAGTT
LPL	FWD GTCCGTGGCTACCTGTCATT
	REV TGTCCCACCAGTTTGGTGTA
C/EBPα	FWD AAACAACGCAACGTGGAGA
	REV GCGGTCATTGTCACTGGTC
PPARγ2	FWD CCTATTGACCCAGAAAGCGATT
	REV CATTACGGAGAGATCCACGGA
GAPDH	FWD CACCATCTTCCAGGAGCGAG
	REV TCACGCCACAGTTTCCCGGA
UBC	FWD ATTTGGGTCGCGGTTCTTG
	REV TGCCTTGACATTCTCGATGGT

finger protein 638; NF1 , Neurofibromin 1; ADD1, Adipocyte Determination and Differentiation-dependent factor 1; SREBP1, Sterol Regulatory Element-binding Protein 1; CREB, Cyclic AMP Response Element-binding protein; KLFs, Kruppel-like Factors; GATA, GATA binding protein; PREF-1, Preadipocyte Factor-1; SIRT1, Histone deacetylase Sirtuin 1; TAZ, Transcriptional-coactivator with PDZ-binding motif; Krox20, EGR C2H2-type zinc-finger protein; FABP4, Fatty Acid Binding Protein 4; FAS, Fatty Acid Synthase; LPL, Lipoprotein Lipase; SCD, Stearyl-CoA-Desaturase; GLUT-4, Glucose transporter 4; C2H2-ZF, Cys2-His2 zinc fingers; WISP2, WNT1 Inducible Signaling Pathway Protein 2; BMP4 , Bone Morphogenetic Protein 4; UBC, Ubiquitin C; IRES, Intra-Ribosomal Entry Site; eGFP, Enhanced Green Fluorescent Protein; LDs, Lipid Droplets; PPRE, PPAR-Responsive Element; ACOX1, Acyl-CoA Oxidase 1; DEX, Dexamethasone; IBTX, Isobutyl-methylxanthine; BmMSCs, Bone marrow Mesenchymal Stem Cells; Runx2 , Runt-related transcription factor 2; Smad, Small mother against decapentaplegic; NuRD, Nucleosome Remodeling Deacetylase; PDGFR-α, Platelet-Derived Growth Factor Receptor –α; HDAC, Histone Deacetylase; GAPDH, Glyceraldehyde 3-Phosphate Dehydrogenase

References

1. Schaffler, A., & Buchler, C. (2007). Concise review: Adipose tissue-derived stromal cells-basic and clinical implications for novel cell-based therapies. *Stem Cells, 25*, 818–827.
2. Zhu, Z. H., Song, W. Q., Zhang, C. Q., & Yin, J. M. (2016). Dimethyloxaloylglycine increases bone repair capacity of adipose-derived stem cells in the treatment of osteonecrosis of the femoral head. *Experimental and Therapeutic Medicine, 12*, 2843–2850.
3. Bunnell, B. A., Flaat, M., Gagliardi, C., Patel, B., & Ripoll, C. (2008). Adipose-derived stem cells: Isolation, expansion and differentiation. *Methods, 45*, 115–120.
4. Lefterova, M. I., & Lazar, M. A. (2009). New developments in adipogenesis. *Trends in Endocrinology and Metabolism, 20*, 107–114.
5. Lee, J. E., & Ge, K. (2014). Transcriptional and epigenetic regulation of PPARgamma expression during adipogenesis. *Cell & Bioscience*. https://doi.org/10.1186/2045-3701-4-29.
6. Moseti, D., Regassa, A., & Kim, W. K. (2016). Molecular regulation of Adipogenesis and potential anti-Adipogenic bioactive molecules. *International Journal of Molecular Sciences*. https://doi.org/10.3390/ijms17010124.
7. Mueller, E. (2014). Understanding the variegation of fat: Novel regulators of adipocyte differentiation and fat tissue biology. *Biochimica et Biophysica Acta, 1842*, 352–357.
8. Siersbaek, M. S., Loft, A., Aagaard, M. M., et al. (2012). Genome-wide profiling of peroxisome proliferator-activated receptor gamma in primary epididymal, inguinal, and brown adipocytes reveals depot-selective binding correlated with gene expression. *Molecular and Cellular Biology, 32*, 3452–3463.
9. Cristancho, A. G., & Lazar, M. A. (2011). Forming functional fat: A growing understanding of adipocyte differentiation. *Nature Reviews. Molecular Cell Biology, 12*, 722–734.
10. Gustafson, B., Hedjazifar, S., Gogg, S., Hammarstedt, A., & Smith, U. (2015). Insulin resistance and impaired adipogenesis. *Trends in Endocrinology and Metabolism, 26*, 193–200.
11. Gupta, R. K., Arany, Z., Seale, P., et al. (2010). Transcriptional control of preadipocyte determination by Zfp423. *Nature, 464*, 619–623.
12. Hammarstedt, A., Hedjazifar, S., Jenndahl, L., et al. (2013). WISP2 regulates preadipocyte commitment and PPARgamma activation by BMP4. *Proceedings of the National Academy of Sciences of the United States of America, 110*, 2563–2568.
13. Bond, H. M., Mesuraca, M., Carbone, E., et al. (2004). Early hematopoietic zinc finger protein (EHZF), the human homolog to mouse Evi3, is highly expressed in primitive human hematopoietic cells. *Blood, 103*, 2062–2070.
14. Bond, H. M., Mesuraca, M., Amodio, N., et al. (2008). Early hematopoietic zinc finger protein-zinc finger protein 521: A candidate regulator of diverse immature cells. *The International Journal of Biochemistry & Cell Biology, 40*, 848–854.
15. Mega, T., Lupia, M., Amodio, N., et al. (2011). Zinc finger protein 521 antagonizes early B-cell factor 1 and modulates the B-lymphoid differentiation of primary hematopoietic progenitors. *Cell Cycle, 10*, 2129–2139.
16. Mesuraca, M., Chiarella, E., Scicchitano, S., et al. (2015). EBF1 Antagonists of Potential Relevance in B-Lymphoid Malignancies. Biomed Res Int, doi: https://doi.org/10.1155/2015/165238.
17. Yamasaki, N., Miyazaki, K., Nagamachi, A., et al. (2010). Identification of Zfp521/ZNF521 as a cooperative gene for E2A-HLF to develop acute B-lineage leukemia. *Oncogene, 29*, 1963–1975.
18. Salerno, L., Cosentino, C., Morrone, G., & Amato, F. (2015). Computational modeling of a transcriptional switch underlying B-lymphocyte lineage commitment of hematopoietic multipotent cells. *PLoS One*. https://doi.org/10.1371/journal.pone.0132208.
19. Hiratsuka, T., Takei, Y., Ohmori, R., et al. (2016). ZFP521 contributes to pre-B-cell lymphomagenesis through modulation of the pre-B-cell receptor signaling pathway. *Oncogene, 35*, 3227–3238.
20. Sera, Y., Yamasaki, N., Oda, H., et al. (2016). Identification of cooperative genes for E2A-PBX1 to develop acute lymphoblastic leukemia. *Cancer Science, 107*, 890–898.
21. Kamiya, D., Banno, S., Sasai, N., et al. (2011). Intrinsic transition of embryonic stem-cell differentiation into neural progenitors. *Nature, 470*, 503–509.
22. Shen, S., Pu, J., Lang, B., & McCaig, C. D. (2011). A zinc finger protein Zfp521 directs neural differentiation and beyond. *Stem Cell Research*. https://doi.org/10.1186/scrt61.
23. Shahbazi, E., Moradi, S., Nemati, S., et al. (2016). Conversion of human fibroblasts to stably self-renewing neural stem cells with a single zinc-finger transcription factor. *Stem Cell Reports, 6*, 539–551.
24. Spina, R., Filocamo, G., Iaccino, E., et al. (2013). Critical role of zinc finger protein 521 in the control of growth, clonogenicity and tumorigenic potential of medulloblastoma cells. *Oncotarget, 4*, 1280–1292.
25. Liu, T. M., & Lee, E. H. (2013). Transcriptional regulatory cascades in Runx2-dependent bone development. *Tissue Engineering. Part B, Reviews, 19*, 254–263.
26. Hesse, E., Saito, H., Kiviranta, R., et al. (2010). Zfp521 controls bone mass by HDAC3-dependent attenuation of Runx2 activity. *The Journal of Cell Biology, 191*, 1271–1283.
27. Wu, M., Hesse, E., Morvan, F., et al. (2009). Zfp521 antagonizes Runx2, delays osteoblast differentiation in vitro, and promotes bone formation in vivo. *Bone, 44*, 528–536.
28. Addison, W. N., Fu, M. M., Yang, H. X., et al. (2014). Direct transcriptional repression of Zfp423 by Zfp521 mediates a bone morphogenic protein-dependent osteoblast versus adipocyte lineage commitment switch. *Molecular and Cellular Biology, 34*, 3076–3085.
29. Correa, D., Hesse, E., Seriwatanachai, D., et al. (2010). Zfp521 is a target gene and key effector of parathyroid hormone-related peptide signaling in growth plate chondrocytes. *Developmental Cell, 19*, 533–546.
30. Mesuraca, M., Galasso, O., Guido, L., et al. (2014). Expression profiling and functional implications of a set of zinc finger proteins, ZNF423, ZNF470, ZNF521, and ZNF780B, in primary osteoarthritic articular chondrocytes. Mediators Inflamm., doi: https://doi.org/10.1155/2014/318793.

31. Kang, S., Akerblad, P., Kiviranta, R., Gupta, R. K., Kajimura, S., & Griffin, M. J. (2012). Regulation of early adipose commitment by Zfp521. *PLoS Biology*. https://doi.org/10.1371/journal.pbio.1001433.

32. Tseng, K. Y., & Lin, S. (2015). Zinc finger factor 521 enhances adipogenic differentiation of mouse multipotent cells and human bone marrow mesenchymal stem cells. *Oncotarget, 6*, 14874–14884.

33. Kiviranta, R., Yamana, K., Saito, H., et al. (2013). Coordinated transcriptional regulation of bone homeostasis by Ebf1 and Zfp521 in both mesenchymal and hematopoietic lineages. *The Journal of Experimental Medicine, 210*, 969–985.

34. Leuci, V., Gammaitoni, L., Capellero, S., et al. (2009). Efficient transcriptional targeting of human hematopoietic stem cells and blood cell lineages by lentiviral vectors containing the regulatory element of the Wiskott-Aldrich syndrome gene. *Stem Cells, 27*, 2815–2823.

35. Chiarella, E., Carrà, G., Scicchitano, S., et al. (2014). UMG Lenti: Novel lentiviral vectors for efficient transgene- and reporter gene expression in human early hematopoietic progenitors. *PLoS One*. https://doi.org/10.1371/journal.pone.0114795.

36. Akerblad, P., Lind, U., Liberg, D., Bamberg, K., & Sigvardsson, M. (2002). Early B-cell factor (O/E-1) is a promoter of adipogenesis and involved in control of genes important for terminal adipocyte differentiation. *Molecular and Cellular Biology, 22*, 8015–8025.

37. Hesslein, D. G., Fretz, J. A., Xi, Y., et al. (2009). Ebf1-dependent control of the osteoblast and adipocyte lineages. *Bone, 44*, 537–546.

38. Jimenez, M. A., Akerblad, P., Sigvardsson, M., & Rosen, E. D. (2007). Critical role for Ebf1 and Ebf2 in the adipogenic transcriptional cascade. *Molecular and Cellular Biology, 27*, 743–757.

39. Kao, C. H., Hsiang, C. Y., & Ho, T. Y. (2012). Assessment of chitosan-affected metabolic response by peroxisome proliferator-activated receptor bioluminescent imaging-guided transcriptomic analysis. *PLoS One*. https://doi.org/10.1371/journal.pone.0034969.

40. Gong, M., Antony, S., Sakurai, R., Liu, J., Iacovino, M., & Rehan, V. K. (2016). Bone marrow mesenchymal stem cells of the intra-uterine growth-restricted rat offspring exhibit enhanced adipogenic phenotype. *International Journal of Obesity, 40*, 1768–1775.

41. Matsubara, E., Sakai, I., Yamanouchi, J., et al. (2009). The role of zinc finger protein 521/early hematopoietic zinc finger protein in erythroid cell differentiation. *The Journal of Biological Chemistry, 284*, 3480–3487.

42. Bernaudo, F., Monteleone, F., Mesuraca, M., et al. (2015). Validation of a novel shotgun proteomic workflow for the discovery of protein-protein interactions: Focus on ZNF521. *Journal of Proteome Research, 14*, 1888–1899.

43. Hesse, E., Kiviranta, R., Wu, M., et al. (2010). Zinc finger protein 521, a new player in bone formation. *Annals of the New York Academy of Sciences, 1192*, 32–37.

44. Sun, C., Berry, W. L., & Olson, L. E. (2017). PDGFRα controls the balance of stromal and adipogenic cells during adipose tissue organogenesis. *Development, 144*, 83–94.

45. Kilroy, G., Burk, D. H., & Floyd, Z. E. (2016). Siah protein mediates early events in commitment to an Adipogenic pathway. *The Journal of Biological Chemistry, 291*, 27289–27297.

46. La Rocca, R., Fulciniti, M., Lakshmikanth, T., et al. (2009). Early hematopoietic zinc finger protein prevents tumor cell recognition by natural killer cells. *Journal of Immunology, 182*, 4529–4537.

47. Misaggi, R., Di Sanzo, M., Cosentino, C., et al. (2014). Identification of H ferritin-dependent and independent genes in K562 differentiating cells by targeted gene silencing and expression profiling. *Gene, 535*, 327–335.

48. Codispoti, B., Rinaldo, N., Chiarella, E., et al. (2017). Recombinant TAT-BMI-1 fusion protein induces ex vivo expansion of human umbilical cord blood-derived hematopoietic stem cells. *Oncotarget, 8*, 43782–43798.

Affiliations

Emanuela Chiarella[1] · **Annamaria Aloisio**[1] · **Bruna Codispoti**[2] · **Giovanna Nappo**[3] · **Stefania Scicchitano**[1] · **Valeria Lucchino**[1] · **Ylenia Montalcini**[1] · **Augusto Camarotti**[4] · **Olimpio Galasso**[5] · **Manfredi Greco**[6] · **Giorgio Gasparini**[5] · **Maria Mesuraca**[1] · **Heather Mandy Bond**[1] · **Giovanni Morrone**[1]

[1] Laboratory of Molecular Haematopoiesis and Stem Cell Biology, University Magna Græcia, Catanzaro, Italy

[2] Tecnologica Research Institute- Marrelli Hospital, Crotone, Italy

[3] UCSF Hellen Diller Cancer Center, University of California, San Francisco, CA, USA

[4] Federal University of Paraíba (UFPB), João Pessoa, Brazil

[5] Department of Orthopaedic & Trauma Surgery, University "Magna Graecia", Catanzaro, Italy

[6] Department of Plastic Surgery, University "Magna Graecia", Catanzaro, Italy